Flash Flood Hazard Zone Mapping Using GIS: Sarpang

Jigme Tenzin[1], Aparna S Bhaskar[2]
[1]*Department of Civil Engineering and Surveying,*
Jigme Namgyel Engineering College, Royal University of Bhutan, Dewathang, Bhutan
[2]*Civil Engineering Department, SRM Institute of Science and Technology, Kattankulathur, Chennai, India*

Abstract- Flash flood is an overflow of water that submerge lands and properties affecting lives and habitats all around the world. It is impossible to avoid risk or prevent their occurrence but we can reduce their effects. Incessant monsoon rains in the month of July 2016, triggered flash floods in several southern districts of Bhutan including Sarpang town affecting hundreds of people. The town was also wiped out after an overnight flood in 1996. Hence the present study aims to prepare hazard zone map by modeling flash flood with respect to rainfall by integrating geospatial technology and HEC-RAS hydraulic model. The inundation map was compared with the base map to identify and delineate affected land properties. Rainfall data from Bhutan Hydro Met Department has been used to validate the model from recent flood event. Hazard zone map was validated by the model output where maximum inundation corresponds to higher risk zone.
Keywords – Hazard zone, Flash flood, HEC-RAS, AHP, MCDA

I. INTRODUCTION

Floods can be explained as excess flows exceeding the transporting capacity of river channel, lakes, ponds, reservoirs, drainage system, dam and any other water bodies, whereby water inundates outside water bodies. Flash flood is an integrated effect of high intensity rainfall, sudden breach of lakes, collapse of check dams and very steep topography (Chakrabarty and Mandal 2015). Flooding due to storm events has become a major concern in many regions of the world (Knebl et al. 2004). Flash floods is a subset of floods that is particularly damaging natural hazard worldwide due to their multidisciplinary nature of difficulty in forecasting and fast response that limits emergency responses (Saharia et al. 2016). It gives impact to human lives causing severe economic loss due to damages. Flash flood is affecting people, wildlife and habitats around the world due to climate change resulting cloudburst, melting of snow, glacial lake outburst, high intensity rainfall etc. Of all natural hazards, flood is the most widely distributed natural hazard to life (Alaghmand et al. 2010). As the average temperatures increases globally, the occurrence of severe to extreme weather events increases, and hence, global warming has brought further urgency to the prediction of flood levels and damages (Knebl et al. 2004), there by demonstrating the necessity of dependable flash flood hazard zone maps.

International researchers with Asian Disaster Reduction Centre (ADRC) in 2015 stated that the most recent climate change effect disaster took place in Bhutan (2009 Cyclone Aila precipitated floods), taking 12 lives and causing losses of more than Nu. 700 million. Also stated that flash flood is one of the most common and devastating natural disaster occurs in Bhutan during monsoon (June, July and August.

The heavy rainfall caused the Sarpang River to overflow and flooded Sarpang town on 21 July, 2016 affecting 63 families. Portion of Tsirang Sarpang Highway has also been washed away (Office of the Resident Coordinator Situation Report, 2016). The flood water completely destroyed recently transplanted paddy fields of some 30 households. Sarpang town has faced number of such destruction due to flash flood. The town was also wiped out after an overnight flood in 1996 (Kuensel, 22 July 2016). Flash flood in Sarpang, especially in the downstream part is a combined effect of rainfall in the highlands that goes through tributaries of the main stream. Some literatures suggest that the frequency and magnitude of river flood might increase due to climate change (Getahun and Gebre 2015). Flash flood is a big concern in Sarpang due to human welfare losses and crop damages which stipulates indispensability of flood inundation mapping and hazard assessment. There is a need for flood regulation, timely forecasting and hazard extent mapping in the Sarpang Area.

Vulnerability is increasing because of increases in population, and this varies from place to place, due to a number of factors, indicating the importance of carrying out such studies depending upon the characteristics situations of the study area (Montz and Gruntfest 2002).

Pramojanee et al. (1997) and Alaghmand et al. (2010) has given a definition of hazard as threatening event or the probability of occurrence within a specified period of time and within a given area of potentially damaging phenomena. A studies by Rahmati et al. (2015) on flood hazard zoning in Yasooj region, Iran, using GIS and multi-criteria decision analysis shows that AHP and GIS technique are promising of making rather reliable prediction for

flood extend and can be suggested for assessment of the flood hazard potential, specifically in no-data region. Accuracy of any hydrologic model depends mostly on the accuracy of the DEM used (Lagacherie et al. 1996).

Flood hazard mapping creates easily read, rapidly accessible charts and it is an important component for suitable land use planning in flood risk areas (Gitika and Ranjan 2015). River flood hazard mapping was first initiated in 1988 in the United States by the Hydrologic Engineering Centre (HEC) of the U.S. Army Corps of Engineers (Alaghmand et al. 2010).

Flood risk mapping is an important component for proper urban planning in order to reduce the probability of flood occurrence and also reduce the effect of flood hazard when it occurs (Kaoje 2016). Naturally the areas which have the greatest vulnerability of flooding are the flood plain, the lower river terraces and the downstream plain (Pramojanee et al. 1997).

Getahun and Gebre in 2015 adopted flood generating factors, i.e. slope, elevation, rainfall, drainage density, land use, and soil type to rate and combined to delineate flood hazard zones using a multi-criteria evaluation technique in a GIS environment. The weight of flood generating factors were computed by pair wise comparison for a final weighted overlay analysis to generate the flood hazard map. Their simulation was done for 5, 10, 25, 50 and 100 years return periods and suggested that proper land use management and afforestation, is significant to reduce the adverse effects of flooding particularly in the low-lying flood prone areas.

Nadzri et al. (2015) successfully modelled the watershed area and map showing the flooded areas has been delineated. They geometrically overlaid the flooded area on the topographic map to delineate the affected areas. The inundation flood map generated indicates the spatial distribution of the flooded area which is located at areas with relatively low relief and also pointed out that generally the high water depth occurred along the main channel and spreads gradually to the floodplains.

The Analytic Hierarchy Process (AHP) is a theory of measurement through pairwise comparisons and depends upon the judgements of experts to obtain priority scales (Saaty, 2008). Multi-Criteria Decision Analysis (MCDA) has been recognized as an important tool for analyzing complex decision problems and coupled with GIS approaches have been employed in spatial modelling and natural hazards analysis (Rahmati et al., 2016).

The comparisons were made using a scale of absolute judgements which represents the importance of one elements over another with respect to a given attribute. Quite often the judgements may be inconsistent. Therefore, how to measure inconsistency and improve the judgements, when it is possible to obtain better consistency is a concern of the AHP (Saaty, 2008).

The Analytic Hierarchy Process (AHP) method is widely used in multiple-attribute decision making (Franek and Kresta, 2014). They have compare and discuss the application of various judgment scale and their results presented that Linear (Saaty scale) is still a favorable option. Ouma and Tateishi, (2014) studied on urban flood vulnerability and risk mapping using integrated multi-parametric AHP and GIS and validated the strength of proposed approach.

II. STUDY AREA

The study area watershed is located between 26.71°N and 27.23°N latitudes and 90.01°E and 90.83°E longitudes. It covers an area of 142.89 sq.km and serves as home to about 3000 inhabitants (NSB 2005). The total length of the main stream is about 18 km and it is the principal stream of drainage basin covering major parts of Hiley Geog and some part of Shompangkha region. Land use landcover is mainly dominated by forest cover followed by agriculture land and settlement. The main location covers the Sarpang Town with major affected Market Area. Main cash crop grown are rice and ginger. The communities also depend on livestock rearing for income generation.

The sites fall within tropical to subtropical type of climatic zone with altitudes ranging from about 170 m to 4200 metres above Mean Sea Level (MSL). The sites vary in topography from nearly flat to steep mountainous slopes. Although, screened from the full brunt of the monsoon by the Meghalaya hills in India, southern Bhutan still receives heavy and intense orographic rainfall, with annual mean of 2.5-5 m (Land Use Planning Project, 1994) and mean annual temperature of 16.7 degree Celsius (NSB, 2013). Study area watershed with base map is shown in Fig. 1.

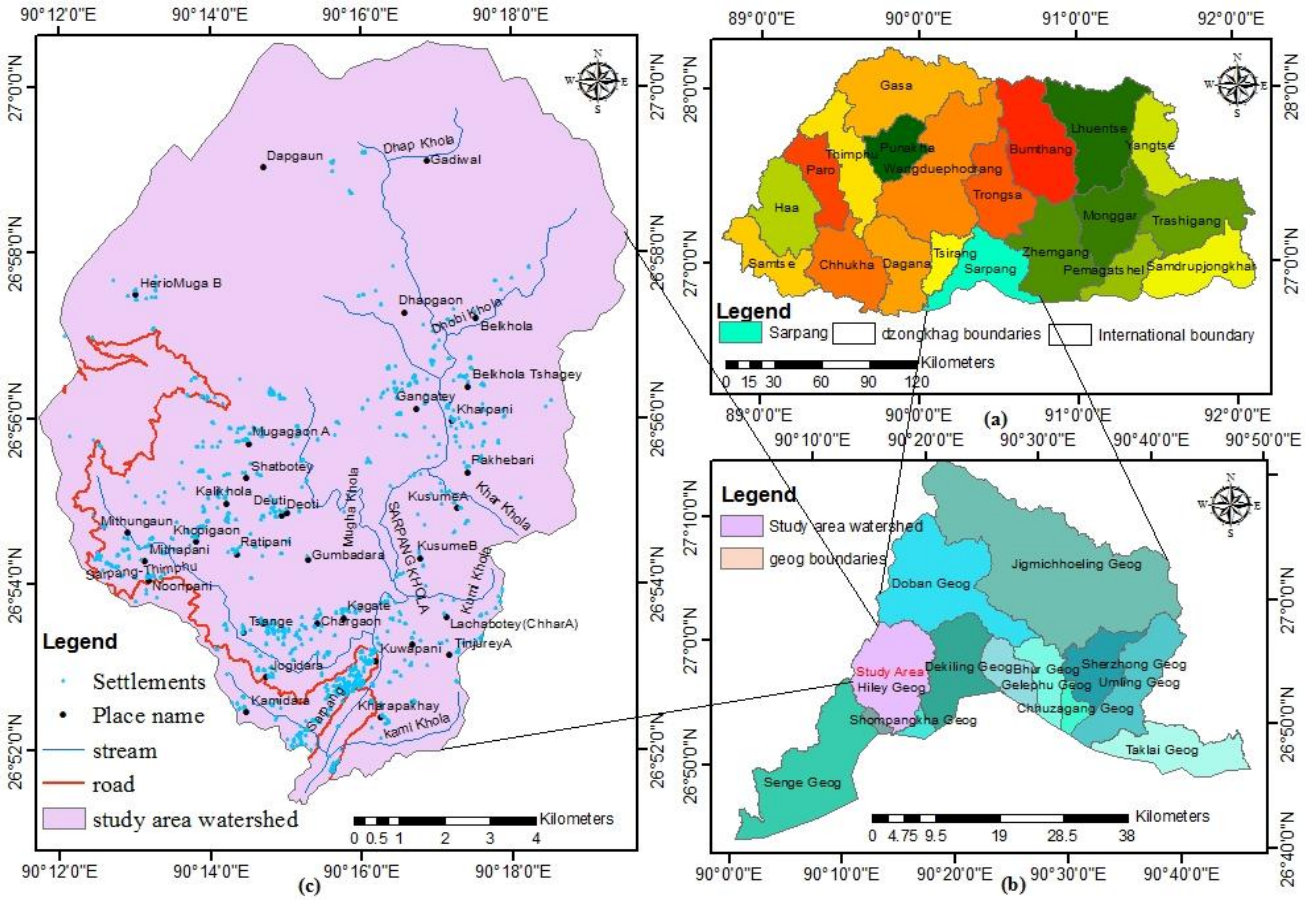

Figure 1. Study area map of Sarpang

II. MATERIALS AND METHODS

SRTM DEM (Shuttle Radar Topographic Mission Digital Elevation Model) of 1arc resolution from USGS has been used as main input data. Landsat 8 OLI was used for landuse landcover classification. Ancillary data like rainfall data from Meteorology Division, Department of Hydromet Services (DHMS), Ministry of Economic Affairs (MoEA), Bhutan, Topographic map from National Land Commission Secretariat (NLCS) and other data from National Statistics Bureau of Bhutan (NSB) were used.

ArcGIS 9.2 was used for mapping and spatial analysis. ArcGIS 9.2 extension HEC-GeoRAS 9.2 and HEC-RAS 5.0.1 (Hydrologic Engineering Centre-River Analysis System) from US Army Corps of Engineers were used for data processing and analysis.

Overall flowchart of the methodology adopted for this study is as shown in the Fig. 2. SRTM DEM was used as base data for overall methodology and processing to generate TIN (Triangulated Irregular Network). The analysis of different hydraulic model to detect flash flood probability using HEC-RAS (Chakrabarty. and Mandal 2015) and combined used of HEC-HMS and HEC-RAS models in GIS in order to simulate flood (Hashemyan et al. 2015) indicates the effectiveness of HEC-RAS models.

Integrated spatial technology of Geographical Information System (GIS) and the HEC-RAS hydraulic model for flood inundation mapping gives good accuracy output (Nadzri et al. (2015). The authors have assumed the flow as steady and uniform flow characteristics while modelling to compute inundation in HEC-RAS as they relate to an open channel.

The studies on Effect of land use-based surface roughness on hydrologic model output says for large watersheds, modelers typically use land use / land cover datasets to assign Manning's n values based on the use or cover class (Alfred et al. 2009). Their results also suggest that the use of (National Land Cover Dataset) NLCD-defined Manning's n values is acceptable for medium to large watersheds.

This study deploys HEC-RAS assist by interfacing ArcGIS extension; HEC-GeoRAS, and ArcGIS. Flood inundation map was generated by incorporating Manning's n values defined by types of channel, slope and landuse landcover of the watershed. It was validated using the information acquired from flash flood historic event of recent past.

MCDA method of AHP technique was used to generate weights and normalized rates of the watershed characteristics to generate flood hazard potential index by WLC techniques assisted by ArcGIS. Flood hazard map was validated by the flash flood model generated.

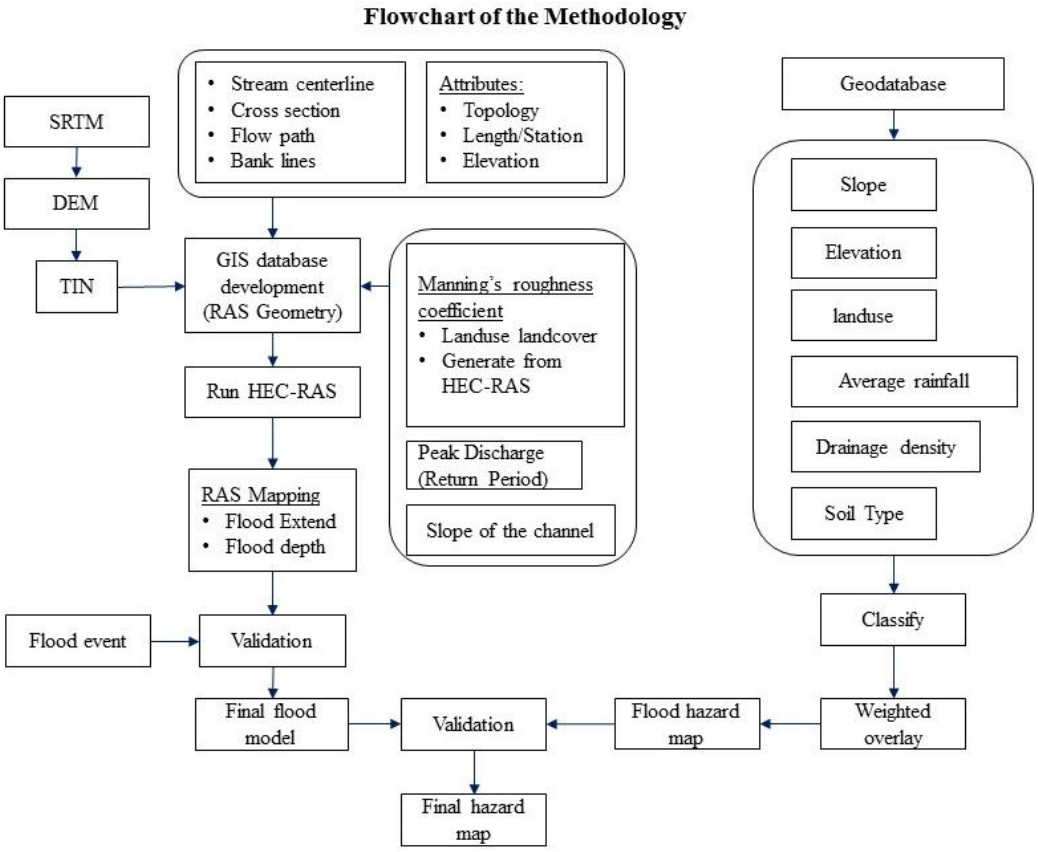

Figure 2. Flow Chart of the Methodology

III. RESULTS AND DISCUSSIONS

3.1 Ras Gepmetric Data Creation

TIN was generated using 3D Analyst Tools in ArcGIS 9.2 by using DEM as an input data. Then RAS geometric data was created by using TIN as base data in RAS Geometry of HEC-GeoRAS. Stream centerlines, bank lines, flow path lines and XS cut lines layers were created and delineated. River reach name and flow path name were also assigned. Finally, stream centerline attributes and XS cut lines attributes were created. Geometric data thus created is shown in Fig. 3 which was exported as RAS data to be used in HEC-RAS.

3.2. Manning's Roughness coefficient

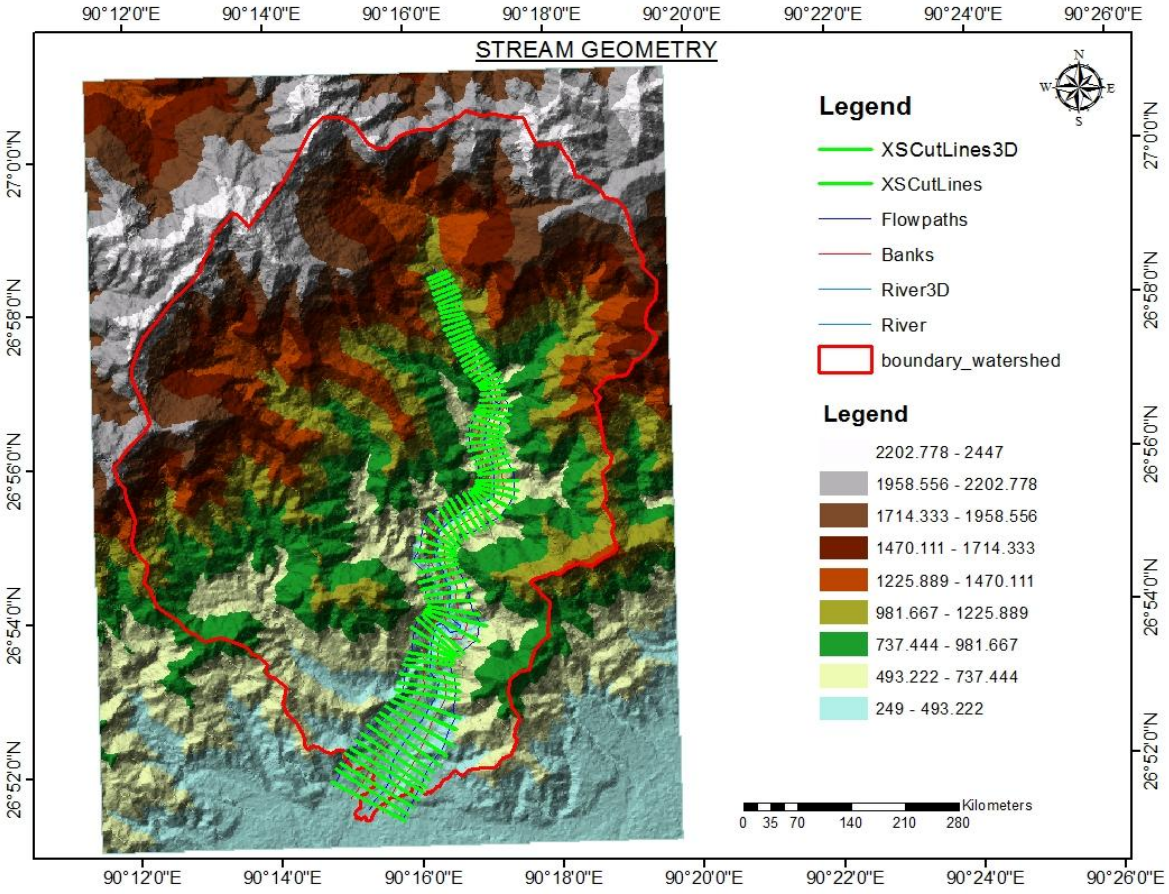

Figure 3. Stream geometry created using TIN

After importing RAS data into HEC-RAS, manning's n values was assigned primarily based on Landuse Landcover from manning's n values used for NLCD map (Alfred et al. 2009), Values of Manning's n for agriculture or overbank areas (Jeff et al. 2006, USGS) and channel type and slope of the channel (McCuen 2004). Taking into consideration the natural earth bottom and rubble side type channel and landuse landcover map generated from Landsat OLI image using ENVI 4.3, manning's n considered for this study is given in Table 1. Geometric data of each station can be viewed and edited if necessary like elevation values.

Slope map of the study area was generated using SRTM DEM data and Spatial Analysis Tools in ArcGIS 9.2. Slope interval of value from 0° to 10° has been assigned.

The low lying location of study area with highest possibility of occurring flash flood were found within 0 to 20 degree slope.

Landsat 8 OLI images of November 19, 2015 from Earth Explorer has been used to generate landuse landcover map. Two images has been mosaicked using ENVI 4.3 and unsupervised isodata classification was applied. Few landuse classes were identified: settlement, forest cover, barren land, fallow lands, and streams. Slope map and LULC map is shown in Fig. 4 and Fig. 5 respectively.

Table 1. Manning's n values

LULC/Channel Type	n values
Barren land	0.0113
Deciduous forest	0.36
Agriculture land	0.35
Earth bottom and rubble side	0.30

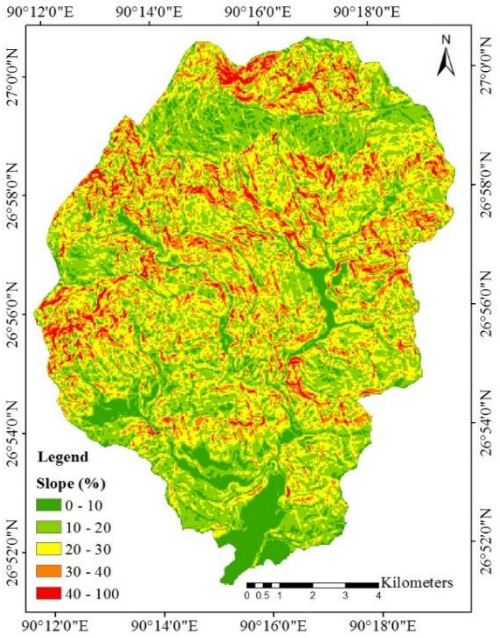

Figure 4. Slope map

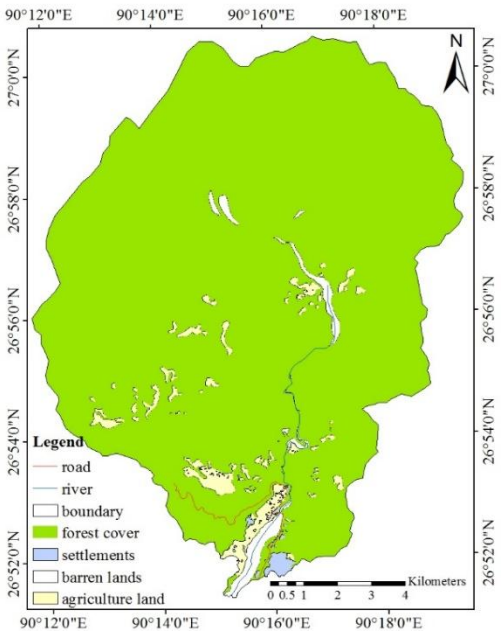

Figure 5. LULC map

3.3. Peak discharge

Steady flow condition was considered for analysis. Peak discharge was assigned based on the calculated average peak discharge value of 21 years rainfall data. Average daily rainfall data (1996-2016) of Sarpang rain gauge station were collected from DHMS, Bhutan and peak discharge was calculated by Kinematic Wave Parameter (KWP) for flow velocity and discharge estimation (Rodriguez-Iturbe et al. 1982) shown in equation 1. Average slope of channel as 0.4 and channel outlet cross section of 600 m2 were calculated from stream profile and stream cross section respectively which were generated in HEC-RAS software.

Discharge (Q = d.B.v) (m3/s) (1)

Where d.B = Cross sectional area (m2)

VΩ = 0.665αΩ0.6 (ir A) 0.4

αΩ = SΩ0.5/nB2/3

Calculated peak discharge ranges from 700 m3 to 1000 m3. Therefore, peak discharge value of 700 m3, 800 m3, 900 m3 and 1000 m3 were given for profile 1(PF1) respectively at different point downstream. Subsequently an increased value was assigned for profile 2 (PF2) and profile 3 (PF3) for further analysis.

3.3.1 Steady flow analysis

Steady flow analysis was done in HEC-RAS software based on open flow channel and sub-critical flow regime. Flow cross section, flow profile and 3D cross section with depth of water were generated.

3.3.2 Inundation mapping

After steady flow analysis being done in HEC-RAS, GIS data was exported and imported into ArcGIS for inundation analysis using RAS Mapping. Imported GIS data need to be converted from SDF format into XML format. Inundation map for different profile with various discharge rate can be mapped and overlay on LULC map to analyze the amount of damages caused to agriculture, settlement, vegetation etc. Inundation and flood extend map for different discharge profile is shown in Fig. 6. Total area of LULC map is shown in Table 2, LULC Area after flooding with different discharge profile in Table 3 and LULC flooded Area of different discharge profile in Table 4 and percentage amount flooded is shown in Table 5.

Table 2. LULC area

Settlement (m2)	Agriculture land (m2)	Forest cover (m2)	Barren land (m2)
653826	4337010.15	135062628.8	2338164.07

Table 3. LULC area after flooding

Profiles	Outlet peak discharge (m3)	Settlement (m2)	Agriculture land (m2)	Forest cover (m2)	Barren land (m2)
Profile 1 (PF1)	1000	651047.42	4231697.94	134351600.7	1312353.54
Profile 2 (PF2)	1500	647624.15	4191456.92	134201389.7	1127712.47
Profile 3 (PF3)	2000	635587.04	4116501.88	133917195.9	942036.21

Table 4. LULC flooded area of different discharge profile

Profiles	Outlet peak discharge (m3)	Settlement (m2)	Agriculture land (m2)	Forest cover (m2)	Barren land (m2)
Profile 1 (PF1)	1000	2778.58	105312.21	711028.08	1025810.53
Profile 2 (PF2)	1500	6201.85	145553.23	861239.11	1210451.6
Profile 3 (PF3)	2000	18238.96	220508.27	1145432.87	1396127.86

Table 5. Percentage of flooded area

Profiles	Outlet peak discharge (m3)	Settlement (%)	Agriculture land (%)	Forest cover (%)	Barren land (%)
(PF1)	1000	0.002	0.074	0.498	0.718
(PF2)	1500	0.004	0.102	0.603	0.847
(PF3)	2000	0.013	0.154	0.802	0.977

3.4. Drainage density

Drainage density is defined as the total length of all the rivers and streams in a drainage basin divided by the total area of the drainage basin. The vector data of streams created was converted to raster of 30 x 30 m grid cell size using conversion tools in ArcGIS. Focal statistics tool under spatial analyst tools was used to map drainage density using raster data as input by considering cells within circular radius of 20 cell. Drainage density map thus created was reclassify as very low density, low density, medium density, high density and very high density of equal interval. Subsequently, it was digitized to get the vector output and finally to calculate the actual drainage density of each class as shown in Table 6. Drainage density map is shown in Fig. 7.

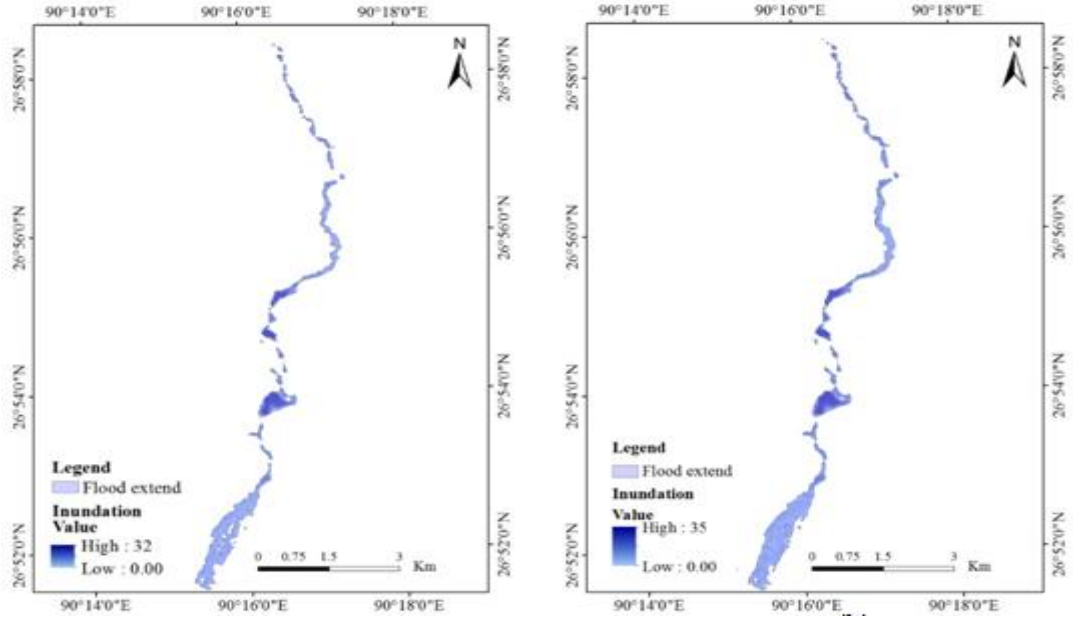

(a) (b)

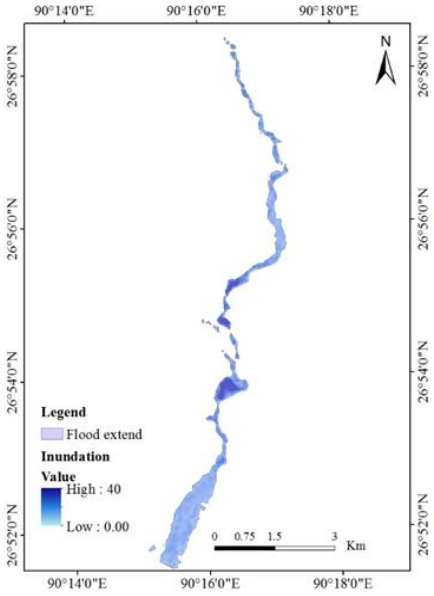

(c)

Figure 6. Flood extend and Inundation map: (a) profile 1, (b) profile 2 and (c) profile 3

Table 6 Drainage density calculation

Drainage Classification	Total length of stream (L) (km)	Total area of basin (A) (km2)	Drainage density (L)/(A) per km
Very low density	6.973	4.667	1.494
Low density	56.020	20.754	2.699
Medium density	77.484	24.831	3.121
High density	212.954	57.835	3.682
Very high density	130.497	34.295	3.805

3.5 Geology

The subsurface geology of the area is one factor that contributes to the way flash flood occurs and essentials to identify its impact. The only available geological map of the study area from Journal of Map (Long et al., 2011) was used. Five different classes of geology were found within the study area as presented in Fig. 8.

3.6 Elevation

Elevation of the area above MSL (Mean Sea Level) was generated from SRTM DEM data and reclassify into five different categories. Literature reviews says that the low elevated places are more susceptible to flooding due to high rainfall accumulation than high elevated places. Elevation map is as shown in Fig. 9.

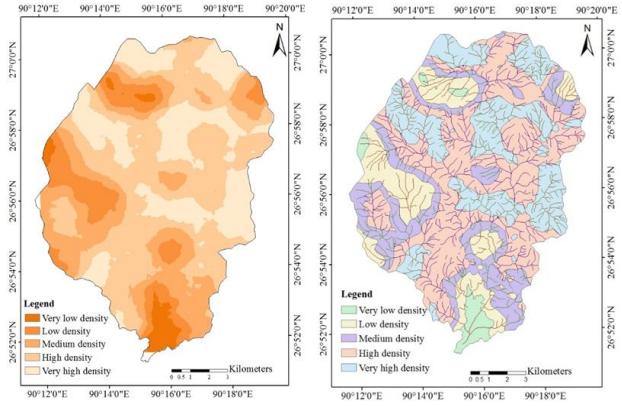

(a) (b)

Figure 7. Drainage density map: (a) raster map and (b) vector map

3.7 Distance from river

Distance from river map was generated by using buffer analysis tools in ArcGIS. The distance of 0-500 m, 500-1000 m, 1000-1500 m, 1500-2000 m and 2000 m and above from the centerline of stream was buffered and mapped. The area closer to the river or stream network may be at higher risk of flooding if only flowing water through stream is considered. However, if high intensity rainfall accounts on larger area, the geomorphological characteristics plays a vital role in determining hazard zone. Distance from river map is shown in Fig. 10.

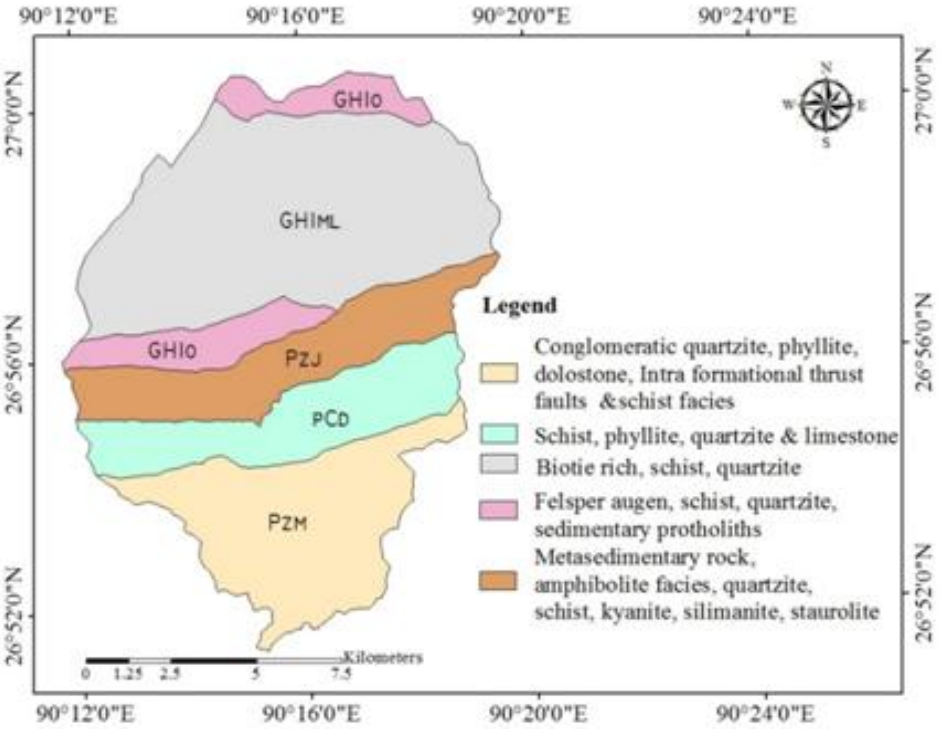

Figure 8. Geology map

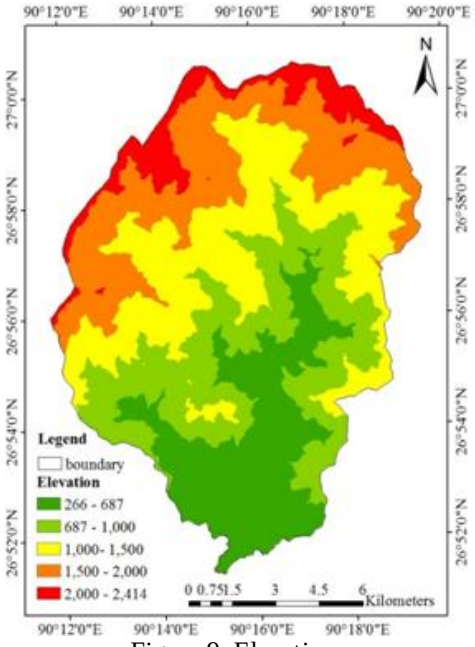

Figure 9. Elevation map

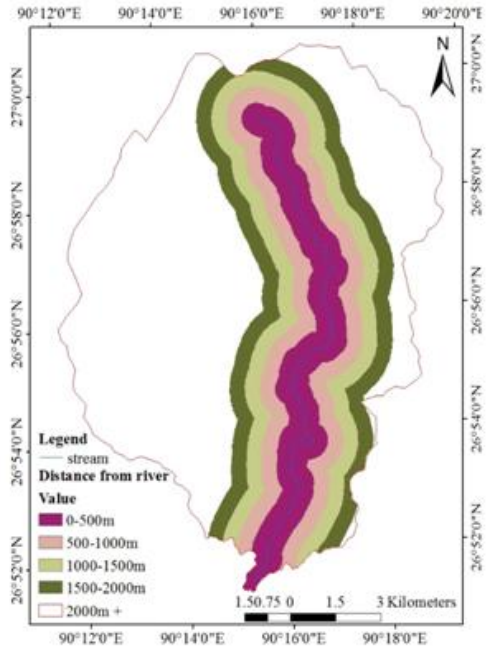

Fig.10 Distance from river map

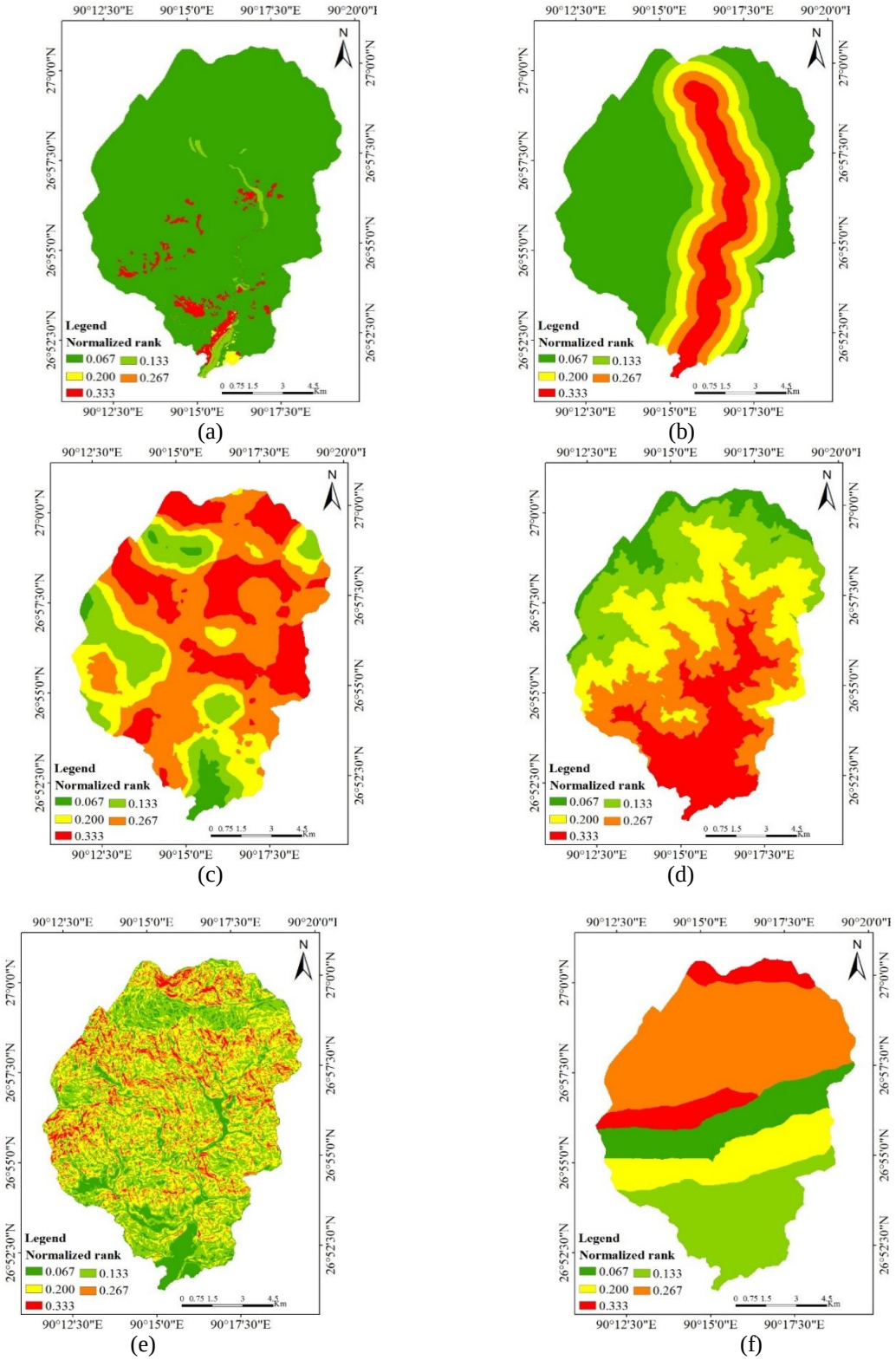

Figure 11. Raster map with normalized rank assigned to each 30 x 30 grid cell: (a) LULC, (b) distance from river, (c) drainage density, (d) elevation, (e) slope and (f) geology

3.8 Rating of Classified Characteristics Factor

Probability rating of flash flooding in every watershed was done by considering certain causative watershed characteristics factor. The comparative significance of each classes was indicated by normalized rank. The causative factors taken into considerations for this study are:

Slope of the watershed
LULC type of the watershed
Drainage density of the watershed
Geology type of the watershed
Elevation of the watershed and
Distance from river

Theoretically, there are a greater number of causative watershed characteristic factors like soil type, geomorphology, population density etc. Considering these parameters and the use of high-resolution data will improve the accuracy of the result. For the data with medium resolution, the output of the study is acceptable.

The normalized rank of each class for all characteristics factor is represented in appendix 1 and raster map with normalized rank assigned to each 30 x 30 grid cell is shown in Fig. 11.

3.9 Weights of the Attributes

To assign a weight of the watershed characteristics attributes, MCDA method was used where AHP techniques of pairwise comparison (Saaty, 1980) was used. Pairwise comparison of the attributes are done based on Saaty's nine point rating scale shown in Table 7. The attributes were arranged in matrix form and comparisons are made to obtained the weight of each attributes until the required consistency ratio of less than 0.1 is achieved, which otherwise the process has to repeat. Here, the consistency ratio was found 0.074 which indicates the most consistent. Watershed characteristics impact prioritization on flash flood is shown is Table 8, Normalized weight calculation in Table 9 and consistency ratio in Table 10.

Table 7. Saaty's rating scale (Saaty, 1980)

Intensity of importance	Definition	Explanation
1	Equal importance	Two factors contribute equally to the objective
3	Somewhat more important	Experience and judgement slightly favor one over the other.
5	Much more important	Experience and judgement strongly favor one over the other.
7	Very much more important	Experience and judgement very strongly favor one over the other. Its importance is demonstrated in practice.
9	Absolutely more important.	The evidence favoring one over the other is of the highest possible validity
2,4,6,8	Intermediate values	When compromise is needed

Table 8. Comparison table

	j						
		Slope	LULC	Distance from river	Altitude	Drainage density	Geology
i	Slope	1	1/4	1/2	1/4	1/3	5
	LULC	4	1	3	4	2	4
	Distance from river	2	1/3	1	2	1/2	3
	Elevation	4	1/4	1/2	1	1 2/5	2
	Drainage density	3	1/2	2	5/7	1	4
	Geology	1/5	1/4	1/3	1/2	1/4	1
	Total	14.20	2.58	7.33	8.46	5.48	19.00

Table 9. Normalized weight calculation

	j								
		Slope	LULC	Distance from river	Altitude	Drainage density	Geology	Sum	Score/weight

	Slope	0.070	0.097	0.068	0.030	0.061	0.263	0.589	0.098
	LULC	0.282	0.387	0.409	0.473	0.365	0.211	2.126	0.354
	Distance from river	0.141	0.129	0.136	0.236	0.091	0.158	0.892	0.149
	Elevation	0.282	0.097	0.068	0.118	0.255	0.105	0.925	0.154
	Drainage density	0.211	0.194	0.273	0.084	0.182	0.211	1.155	0.192
	Geology	0.014	0.097	0.045	0.059	0.046	0.053	0.314	0.052

Table 10. Consistency ration calculation

	j								
i		Slope	LULC	Distance from river	Altitude	Drainage density	Geology	Sum	Sum/score
	Slope	0.098	0.089	0.074	0.039	0.064	0.261	0.625	6.369
	LULC	0.393	0.354	0.446	0.617	0.385	0.209	2.404	6.784
	Distance from river	0.196	0.118	0.149	0.308	0.096	0.157	1.024	6.894
	Elevation	0.393	0.034	0.074	0.154	0.269	0.105	1.029	6.674
	Drainage density	0.294	0.177	0.297	0.110	0.192	0.209	1.280	6.653
	Geology	0.020	0.034	0.050	0.077	0.048	0.052	0.281	5.375
Sum									38.750
$\frac{Mean}{\lambda_{max}}$									6.458
CI									0.092
CR									0.074

If any λmax is less than n, then it indicates an error in the calculation, which is a useful for checking. To calculate Consistency Ratio (CR), formula given by Saaty in equation 2 and equation 3 were used.

$$CR = \frac{CI}{RI} \quad (2)$$

Where CI = consistency index and
RI =Random index
Consistency index was calculated as;

$$CI = \frac{(\lambda_{max} - n)}{n-1} \quad (3)$$

Where λmax = mean of the score calculated
n = number of attributes
Random index value based on n value given by Saaty as shown in Table 11.

Table 11. Random index value (Saaty, 1980)

N	1	2	3	4	5	6	7	8	9	10
Random Index (RI)	0.00	0.00	0.58	0.90	1.12	1.24	1.32	1.41	1.45	1.49

3.10 Flood Hazard Potential Index

Based on multiple flood exposure watershed characteristics detailed above, developed indices: The Flood Hazard Potential Index by Weighted Linear Combination (WLC) method in ArcGIS (Malczewski, 2000). WLC is normally specified in terms of normalized weights of each characteristic as well as normalized rates for all relative options. Therefore, each factor was divided into a number of classes and each class, weighted according to the estimated significance for causing flooding. The spatial data layers were merged if necessary and converted into raster format

(grid cells), throughout the study area, each raster cell was attributed with final scores representing FHPI. Grid cells are of 30 m by 30 m or 0.0009 km2. The FHPI scores of each grid cell in the study area according to multiple indicators of watershed characteristics to flood events was achieved by equation 4. Reclassify and Lookup tools from Data management tools was used for assigning weights to each grid cell.

$$FHPI_i = SLOPE_W SLOPE_{NR} + LULC_W LULC_{NR} + DISTANCE_W DISTANCE_{NR} + ELEVATION_W ELEVATION_{NR} + GEOLOGY_W GEOLOGY_{NR} + DRAINAGE_W DRAINAGE_{NR} \quad (4)$$

3.11 Hazard Zone Map

After assigning FHPI values to each grid cell, final output map was generated which is hazard zone map and again reclassify in five categories according to the hazard risk as very low, low, intermediate, high and very high-risk zone. It was observed that the very high-risk zones lie mostly along the main stream and over agriculture areas and very low risk zones at higher altitude and forest cover areas. The final hazard zone map is shown in Fig. 12. The percentage of different zones covering the study area is as shown in Table 12.

Table 12. Percentage of area covered by different zones

Risk zone	Total area(km2)	Risk area (km2)	Percentage (%)
Very low risk	142.89	30.361	21.25
Low risk	142.89	40.811	28.56
Intermediate risk	142.89	34.970	24.47
High risk	142.89	26.185	18.33
Very high risk	142.89	10.563	7.39

3.12 Validation

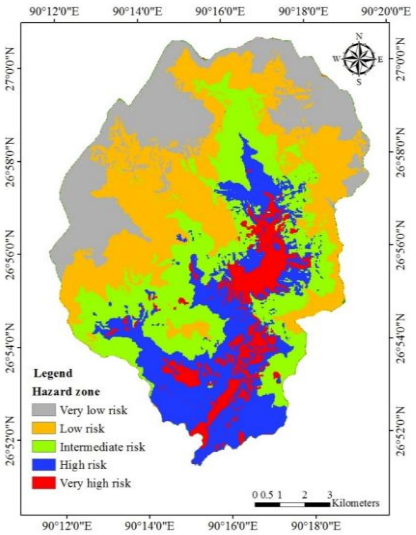

Fig 12 Hazard zone map

The hazard zone map was validated with the flood extend map and inundation map generated. The areas with maximum inundation are found with higher risk zone areas and low inundation with lesser risk zone areas.

IV. CONCLUSION

Flood is a major problem all around the globe due to climate change and the impact of flash flood on human and other inhabitants is catastrophic. Sarpang is one of the developing places with such unavoidable circumstances occurring frequently over the years. Therefore, hazard zone map generated with acceptable accuracy from this study can be used to implement strategic plans to minimize the effect. This also indicates the effectiveness of hazard zone mapping in mountainous terrain landscape like Sarpang and can be replicate to other area of similar characteristics.

In profile 1 analysis of the flash flood model with 1000 m3 outlet peak discharge, which is the current situation of the study area, 0.002% of total settlement, 0.074% of total agriculture land, 0.498% of total forest cover and 0.718% of total barren land were possibly washed away by flash flood. This includes mostly the low-lying areas along the side of streams and some part of Tsirang Sarpang highway road. 0.002% of the settlements are those of Sarpang

vegetable market area including immigration check post. Major agriculture land affected lies below Tsirang Sarpang highway and areas above are found safe.

From the inundation and flood extend analysis, it is observed very crucial to completely relocate the vegetable market and nearby immigration check post. Construction of embankment to protect agriculture land below highway is highly recommended.

With increase in outlet peak discharge for profile 2 and profile 3 aiming at future prediction of similar kind, proportionate increase in flooded area were observed. If any, in future if rainfall intensity increases with outlet discharge as assumed, necessary warning system and evacuation processes have to be kept ready.

From the hazard zone map, it was observed that the very high-risk zones lie mostly along the main stream and over agriculture areas and very low risk zones at higher altitude and forest cover areas. The areas with maximum inundation are found with higher risk zone areas and low inundation with lesser risk zone areas. From the total area of 142.89 km2, 21.25% falls within very low risk zone, 28.56% within low risk zone, 24.47% within intermediate risk zone, 18.33% within high risk zone and 7.39% within very high-risk zone. Hilleygaon agriculture land, some portion of vegetable market, Kuwapani, Kusume, Kharpani, Gangatey, Laring and Tsange are within very high-risk zone. Therefore, the decision makers should focus on this place for further sustainable development plans. The suitable new location for vegetable market could be Kamidata, Jogidara and Chargaon.

V. REFERENCES

[1] Alaghmand, S., Abdullah, R., Abustan, I. and Vosoogh, B., 2013. GIS-based River Flood Hazard Mapping in Urban Area (A Case Study in Kayu Ara River Basin, Malaysia). International Journal of Engineering and Technology, 2(6), 488-500.

[2] Chakrabarty A, Mandal S., 2015. Gis Based Flash Flood Runoff Simulation Model of Upper Teesta River Basin-Using Aster Dem and Meteorological Data. ICDEM 2015: 18th international Conference on Disaster and Emergency Management.

[3] Alfred, J. and Kalyanapu, S. J., 2009. Effect of land use-based surface roughness on hydrologic model output. Journal of Spatial Hydrology, 9(2), 51-71.

[4] Bajabaa, S., Masoud, M. and Al-Amri, N., 2014. Flash flood hazard mapping based on quantitative hydrology, geomorphology and GIS techniques (case study of Wadi Al Lith, Saudi Arabia). Arabian Journal of Geoscience, 7, 2469–2481. doi:10.1007/s12517-013-0941-2

[5] Chakrabarty, S. P., 2016. Flash flood risk assessment for upper Teesta river basin: using the hydrological modeling system (HEC-HMS) software. Model. Earth Syst. Environ.

[6] Colby, J. D., Mulcahy, K. A. and Wang, Y., 2000. Modeling flooding extent from Hurricane Floyd in the coastal plains of North Carolina. Environmental Hazards, 2(4), 157-168.

[7] Elkhrachy, I., 2015. Flash Flood Hazard Mapping Using Satellite Images and GIS Tools: A case study of Najran City, Kingdom of Saudi Arabia (KSA). The Egyptian Journal of Remote Sensing and Space Sciences, 18(2), 261-278.

[8] Franek, J. and Kresta, A., 2014. "Judgment Scales and Consistency Measure in AHP". Procedia Economics and Fina, 14, 164-173.

[9] Gary W. Brunner, John C. Warner, Brent C. Wolfe, Steven S. Piper, and Landon Marston., 2016. HEC-RAS, River Analysis System Applications Guide. Davis: US Army Corps of Engineers Hydrologic Engineering Center (HEC).

[10] Getahun, G., 2015. Flood Hazard Assessment and Mapping of Flood Inundation Area of the Awash River Basin in Ethiopia using GIS and HEC-GeoRAS/HEC-RAS Model. Civil & Environmental Engineering, 5(4),5:179.

[11] Gitika, T., and Ranjan, S., 2016. GIS-based Food Hazard Mapping: A Case Study in Krishnai River Basin, India. Research Journal of Recent Sciences, 5, 50-59.

[12] Hashemyan, F., Khaleghi and Kamyar., 2015. Combination of HEC-HMS and HEC-RAS models in GIS in order to Simulate Flood (Case study: Khoshke Rudan River in Fars Province, Iran). Research Journal of Recent Sciences, 4(8), 122-127.

[13] Kaoje, I. U., 2016. Application of Geographical Information System Techniques in Urban Flood Risk Assessment and Vulnerability Mapping-A Case Study of Cardiff, Wales. International Journal of Scientific and Research Publications, 6(6), 136-149.

[14] Khaleghi, S., Mahmoodi, M., Karimzadeh, S., 2015. Integrated Application of HEC-RAS and GIS and RS for Flood Risk Assessment in Lighvan Chai River. International Journal of Engineering Science Invention, 4(4), 38-45.

[15] Knebl, M. R., Yang, Z. L., Hutchison, K. and Maidment, D. R., 2005. Regional Scale Flood Modeling Using NEXRAD Rainfall, GIS, and HEC-HMS/RAS: A Case Study for the San Antonio River Basin Summer 2002 Storm Event. Journal of Environmental Management, 75, 325-336.

[16] Long, S., McQuarrie, N., Tobgay, T., Rose, C., Gehrels, G. and Grujic, D., 2011. "Tectonostratigraphy of the Lesser Himalaya of Bhutan: Implications for the Along-strike Stratigraphic Continuity of the Northern Indian Margin". Geological Society of America Bulletin, 123(7/8), 1406–1426. DOI:10.1130/B30202.1.

[17] Mohd, N. M. and Reba, M. K., 2015. Integration of GIS and HEC-RAS Hydraulic Model for Flood Inundation Mapping in Sungai su Basin. Geoscience and Digital Earth Centre (INSTeG).

[18] Montz, B. E., & Gruntfest, E., 2011. Flash Flood Mitigation: Recommendations for Research and Applications. Environmental Hazards, 4(1), 15-22.

[19] Rahmati, O., Zeinivand, H. and Besharat, M., 2016. Flood Hazard Zoning in Yasooj Region, Iran, Using GIS and Multi-criteria Decision Analysis. Geomatics, Natural Hazards and Risk, 7(3),1000-1017.

[20] Pokhrel, N. (2016, July 22). Kuensel. Retrieved from kuenselonline: http://www.kuenselonline.com/flood-destroys-sarpang-town/

[21] Pramojanee, P., Tanavud, C., Yongchalermchai, C. and Navanugraha, C. An Application of GIS for Mapping of Flood Hazard and Risk Area in Nakorn Sri Thammarat Province, South of Thailand. Walailak University, Prince of Songkla University.

[22] Saharia, M., Kirstetter, P., Vergara, H., Gourley, J. J., Hong, Y., and Giroud, M., 2016. Mapping Flash Flood Severity in the United States. Journal of Hydrometeorology.

[23] Yang, X. and Rystedt, B., 2002. Predicting Flood Inundation and Risk Using GIS and Hydrodynamic Model: A Case Study at Eskilstuna, Sweden. Indian Cartographer, 183-191.